

Task-space Tracking Control for Dual-arm Free-floating Space Manipulators with Disturbances and Uncertainties

Qian Sun

The Seventh Research Division and the Center for Information and Control, School of Automation Science and Electrical Engineering, Beihang University (BUAA),
Beijing, 100191, P.R.China

Yingmin Jia*

The Seventh Research Division and the Center for Information and Control, School of Automation Science and Electrical Engineering, Beihang University (BUAA),
Beijing, 100191, P.R.China
E-mail: mssunqian@buaa.edu.cn, ymjia@buaa.edu.cn

Abstract

This paper investigates task-space tracking control for dual-arm free-floating space manipulators (DFFSM) subject to unknown disturbances, kinematic and dynamic uncertainties. First, we design a sliding mode disturbance observer to compensate for the lumped disturbances, including unknown disturbances and dynamic uncertainties. Then, an adaptive dynamic surface controller (ADSC) is proposed for DFFSM system, where the uncertain kinematics is estimated by an adaptive algorithm. It is validated through Lyapunov analysis that the tracking errors of the end-effectors are uniformly ultimately bounded under the proposed control scheme. Numerical simulations validate the effectiveness of the proposed control scheme.

Keywords: Dual-arm free-floating space manipulator, Task space, Disturbance observer, Dynamic surface control

1. Introduction

In recent years, space manipulators have increasingly replaced or assisted astronauts in performing various on-orbit servicing. Compared to single-arm space manipulators, DFFSM hold enhanced flexibility and operational capability, making them widely utilized in complex space missions. Therefore, they have attracted significant attention in the field of aerospace technology [1].

The task-space tracking control for DFFSM aims to drive the end-effector of each arm to track a desired trajectory. However, DFFSM are subject to disturbances and uncertainties in space environment, requiring the designed controller with strong robustness. Some researchers have focused on robust tracking control for dual-arm space manipulators [2], [3], [4], [5], [6]. Shi et al. [2], [3] investigated the coordinated control of the base attitude and the manipulator motion in task space, and proposed a sliding mode controller subject to system uncertainties. In [4], an adaptive fuzzy control scheme was developed for grasped dual-arm robots. An approximate Jacobian matrix and a decentralized fuzzy logic system were employed to handle uncertain kinematics and dynamics, and a novel parameter adaptation technique was applied to achieve practical finite-time convergence in the estimation of kinematic parameters and fuzzy logic weights. Aiming to capture a spinning spacecraft with a dual-arm

space robot, Cheng et al. [5] constructed a recurrent fuzzy neural network to approximate the uncertain inertial parameters. Then, a coordinated stabilization control strategy with H_∞ tracking characteristics was then proposed for the post-capture phase. Based on predefined-time stability theory, Liu et al. [6] designed a general nonsingular terminal sliding mode control law for DFFSM subject to persistent disturbances. Despite these achievements, robust tracking control for DFFSM in task space remains limited, which requires further investigation.

Motivated by the discussions above, this paper investigates a disturbance observer-based ADSC for DFFSM. A sliding mode disturbance observer is designed to compensate for unknown disturbances and dynamic uncertainties, while an adaptive law is established to estimate the kinematic uncertainties. The proposed control scheme ensures the uniformly ultimate boundedness of the tracking errors in task space.

2. Main Results

2.1. Kinematics and Dynamics for DFFSM

The DFFSM system includes a base spacecraft and two n -degrees-of-freedom (n -DOF) manipulators, as shown in Fig. 1. The kinematic model of the DFFSM is given by

$$\begin{bmatrix} \dot{\mathbf{x}}_e^a \\ \dot{\mathbf{x}}_e^b \end{bmatrix} = \mathbf{J}_g(\mathbf{x}_b, \mathbf{q}^i, m, \mathbf{I}) \begin{bmatrix} \dot{\mathbf{q}}^a \\ \dot{\mathbf{q}}^b \end{bmatrix}, \quad (1)$$

* Corresponding author.

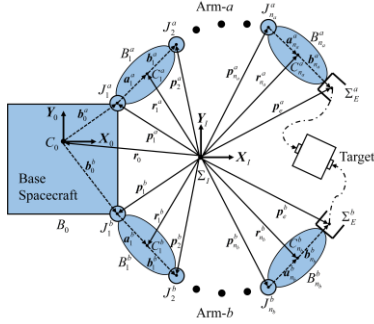


Fig.1 General Structure of DFFSM

where $\dot{\mathbf{x}}_e^i \in \mathbf{R}^{n_i}$ ($i = a, b$) denotes the velocity and angular velocity of the end-effector of Arm- i , $\mathbf{q}^i \in \mathbf{R}^{n_i}$ is the generalized coordinate vector of Arm- i with n_i -DOF, $\mathbf{J}_g \in \mathbf{R}^{(n_a+n_b) \times (n_a+n_b)}$ is the generalized Jacobian matrix of the DFFSM. Using Lagrange method, a reduce-order form dynamic model of DFFSM is derived as

$$\mathbf{M}(\mathbf{q})\ddot{\mathbf{q}} + \mathbf{C}(\mathbf{q}, \dot{\mathbf{q}})\dot{\mathbf{q}} = \boldsymbol{\tau} + \mathbf{d}, \quad (2)$$

where $\mathbf{q} = [(\mathbf{q}^a)^T, (\mathbf{q}^b)^T]^T$, $\boldsymbol{\tau} = [(\boldsymbol{\tau}^a)^T, (\boldsymbol{\tau}^b)^T]^T \in \mathbf{R}^{n_a+n_b}$, $\boldsymbol{\tau}^i \in \mathbf{R}^{n_i}$ is the control input torque, $\mathbf{d} \in \mathbf{R}^{n_a+n_b}$ is the unknown disturbances, and $\mathbf{M}(\mathbf{q})$, $\mathbf{C}(\mathbf{q}, \dot{\mathbf{q}})$ are the inertia matrix and the centrifugal and Coriolis matrix, where

$$\mathbf{C}(\mathbf{q}, \dot{\mathbf{q}}) = \dot{\mathbf{M}}(\mathbf{q})\dot{\mathbf{q}} - \frac{\partial}{\partial \mathbf{q}} \left(\frac{1}{2} \dot{\mathbf{q}}^T \mathbf{M}(\mathbf{q}) \dot{\mathbf{q}} \right).$$

In general, the kinematics and dynamics of DFFSM are uncertain due to the complicated structures. The dynamic uncertainties can be described as

$$\begin{cases} \mathbf{M}(\mathbf{q}) = \mathbf{M}_0(\mathbf{q}) + \Delta\mathbf{M}(\mathbf{q}), \\ \mathbf{C}(\mathbf{q}, \dot{\mathbf{q}}) = \mathbf{C}_0(\mathbf{q}, \dot{\mathbf{q}}) + \Delta\mathbf{C}(\mathbf{q}, \dot{\mathbf{q}}), \end{cases} \quad (3)$$

where $\mathbf{M}_0(\mathbf{q})$ and $\mathbf{C}_0(\mathbf{q}, \dot{\mathbf{q}})$ represent the nominal parts, $\Delta\mathbf{M}(\mathbf{q})$ and $\Delta\mathbf{C}(\mathbf{q}, \dot{\mathbf{q}})$ are the unknown perturbed parts. Substituting (3) into (2), one has

$$\mathbf{M}_0(\mathbf{q})\ddot{\mathbf{q}} + \mathbf{C}_0(\mathbf{q}, \dot{\mathbf{q}})\dot{\mathbf{q}} = \boldsymbol{\tau} + \boldsymbol{\delta}, \quad (4)$$

where $\boldsymbol{\delta} = \mathbf{d} - \Delta\mathbf{M}(\mathbf{q})\ddot{\mathbf{q}} - \Delta\mathbf{C}(\mathbf{q}, \dot{\mathbf{q}})\dot{\mathbf{q}}$ denotes the lumped disturbances, which satisfies $\|\boldsymbol{\delta}\| \leq \beta$ and $\|\dot{\boldsymbol{\delta}}\| \leq \beta_d$ with β and β_d being known positive constants.

Property 1. $\mathbf{J}_g \dot{\mathbf{q}}$ can be linearly parameterized to $\boldsymbol{\theta}_k$:

$$\dot{\mathbf{x}}_e = \mathbf{J}_g \dot{\mathbf{q}} = \mathbf{Y}_k(\mathbf{q}, \dot{\mathbf{q}}) \boldsymbol{\theta}_k, \quad (5)$$

where $\dot{\mathbf{x}}_e = [(\dot{\mathbf{x}}_e^a)^T, (\dot{\mathbf{x}}_e^b)^T]^T$, $\boldsymbol{\theta}_k = [\theta_{k1}, \theta_{k2}, \dots, \theta_{kq}]^T \in \mathbf{R}^q$ is a constant parameter, $\mathbf{Y}_k(\square) \in \mathbf{R}^{(n_a+n_b) \times q}$ denotes the kinematic regressor matrix.

Property 2. The matrix $\dot{\mathbf{M}}_0(\mathbf{q}) - 2\mathbf{C}_0(\mathbf{q}, \dot{\mathbf{q}})$ is skew-symmetric, i.e., $\mathbf{v}^T(\dot{\mathbf{M}}_0(\mathbf{q}) - 2\mathbf{C}_0(\mathbf{q}, \dot{\mathbf{q}}))\mathbf{v} = 0$ for all \mathbf{q} , $\dot{\mathbf{q}}$ and $\mathbf{v} \in \mathbf{R}^{n_a+n_b}$.

Property 3. For a given known positive constant c_0 , the matrix $\mathbf{C}_0(\mathbf{q}, \dot{\mathbf{q}})$ satisfies $\mathbf{C}_0(\mathbf{q}, \dot{\mathbf{q}}) \cdot c_0 \|\dot{\mathbf{q}}\|$.

This paper aims at designing a control algorithm $\boldsymbol{\tau}$ for DFFSM system (1) and (2) to track the desired trajectory of the end-effectors $\mathbf{x}_{ed} \in \mathbf{R}^{m_a+m_b}$ in task space subject to unknown disturbances, kinematic and dynamic uncertainties.

2.2. Sliding Mode Disturbance Observer Design

Define a sliding mode surface $\mathbf{s} = \dot{\mathbf{q}} - \dot{\boldsymbol{\xi}}$ with an auxiliary variable $\boldsymbol{\xi} \in \mathbf{R}^{m_a+m_b}$, where $\dot{\boldsymbol{\xi}}$ is obtained by

$$\mathbf{M}_0(\mathbf{q})\dot{\boldsymbol{\xi}} + \mathbf{C}_0(\mathbf{q}, \dot{\mathbf{q}})\dot{\boldsymbol{\xi}} = \boldsymbol{\tau} + \lambda_0 \mathbf{s}, \quad (6)$$

where $\lambda_0 > 0$ is a gain of system (6). The sliding mode disturbance observer is proposed as

$$\begin{cases} \mathbf{M}_0(\mathbf{q})\dot{\hat{\mathbf{s}}} = -\lambda_0 \hat{\mathbf{s}} + \lambda_1 \text{sgn}(\tilde{\mathbf{s}}) + \hat{\boldsymbol{\delta}}, \\ \dot{\hat{\boldsymbol{\delta}}} = \lambda_2 \tilde{\mathbf{s}} + \lambda_3 \boldsymbol{\sigma} + (\beta_d + \lambda_4) \text{sgn}(\boldsymbol{\sigma}), \end{cases} \quad (7)$$

where $\hat{\mathbf{s}}$ and $\hat{\boldsymbol{\delta}}$ denote the estimation of \mathbf{s} and $\boldsymbol{\delta}$, respectively, $\tilde{\mathbf{s}} = \mathbf{s} - \hat{\mathbf{s}}$ is the estimation error of \mathbf{s} , the notation $\boldsymbol{\sigma}$ is defined as $\boldsymbol{\sigma} = \lambda_j \text{sgn}(\tilde{\mathbf{s}})$, λ_j ($j = 2, 3, 4$) is a positive constant to be determined. Combining (2), (6) and (7), the dynamics of the estimation error $\tilde{\mathbf{s}}$ and $\tilde{\boldsymbol{\delta}}$ can be derived into

$$\begin{cases} \mathbf{M}_0(\mathbf{q})\dot{\tilde{\mathbf{s}}} = -\lambda_0 \tilde{\mathbf{s}} - \lambda_1 \text{sgn}(\tilde{\mathbf{s}}) + \tilde{\boldsymbol{\delta}}, \\ \dot{\tilde{\boldsymbol{\delta}}} = -\lambda_2 \tilde{\mathbf{s}} - \lambda_3 \boldsymbol{\sigma} - (\beta_d + \lambda_4) \text{sgn}(\boldsymbol{\sigma}) + \tilde{\boldsymbol{\delta}}, \end{cases} \quad (8)$$

where $\tilde{\boldsymbol{\delta}} = \boldsymbol{\delta} - \hat{\boldsymbol{\delta}}$ is the estimation error of $\boldsymbol{\delta}$.

Theorem 1. Considering the dynamic model (2) and the designed sliding mode disturbance observer (7), if the observer gains are set as $\lambda_0 = c_0 \|\dot{\mathbf{q}}\|$, $\lambda_1 = \beta - \|\tilde{\boldsymbol{\delta}}\| + \bar{\lambda}_1$, $\bar{\lambda}_1 > 0$, and $\lambda_2 < 2\lambda_3$, the estimation error $\tilde{\boldsymbol{\delta}}$ could converge to zero in finite time.

Proof. The proof is divided into the following two steps:
Step 1: We will prove the finite-time convergence of $\tilde{\mathbf{s}}$. Choosing V_1 as a Lyapunov function candidate

$$V_1 = \frac{1}{2} \tilde{\mathbf{s}}^T \mathbf{M}_0(\mathbf{q}) \tilde{\mathbf{s}}. \quad (9)$$

The time derivative of V_1 is given as

$$\begin{aligned} \dot{V}_1 &= \tilde{\mathbf{s}}^T \mathbf{M}_0(\mathbf{q}) \dot{\tilde{\mathbf{s}}} + \frac{1}{2} \tilde{\mathbf{s}}^T \dot{\mathbf{M}}_0(\mathbf{q}) \tilde{\mathbf{s}} \\ &= \tilde{\mathbf{s}}^T [-\lambda_0 \tilde{\mathbf{s}} - \lambda_1 \text{sgn}(\tilde{\mathbf{s}}) + \tilde{\boldsymbol{\delta}}] + \tilde{\mathbf{s}}^T \mathbf{C}_0(\mathbf{q}, \dot{\mathbf{q}}) \tilde{\mathbf{s}} \\ &\quad \cdot -(\lambda_0 - c_0 \|\dot{\mathbf{q}}\|) \tilde{\mathbf{s}}^T \tilde{\mathbf{s}} - (\lambda_1 - \|\tilde{\boldsymbol{\delta}}\|) \|\tilde{\mathbf{s}}\| \\ &\quad \cdot -\bar{\lambda}_1 \|\tilde{\mathbf{s}}\| \cdot -\frac{\sqrt{2}\bar{\lambda}_1}{\sqrt{\lambda_{\max}(\mathbf{M}_0(\mathbf{q}))}} V_1^{\frac{1}{2}}. \end{aligned} \quad (10)$$

From (10), it can be derived that $\tilde{\mathbf{s}} = \dot{\tilde{\mathbf{s}}} = \mathbf{0}$ within a finite time $t_{d1} \leq \sqrt{2\lambda_{\max}(\mathbf{M}_0(\mathbf{q}))} V_1^{1/2}(0) / \bar{\lambda}_1$, where $V_1(0)$ is the initial value of V_1 . Based on the equivalent output injection theory, $\tilde{\boldsymbol{\delta}}$ is equivalent to the term $\lambda_1 \text{sgn}(\tilde{\mathbf{s}})$, i.e., $(\tilde{\boldsymbol{\delta}})_{\text{eq}} = \boldsymbol{\sigma} = \lambda_1 \text{sgn}(\tilde{\mathbf{s}})$.

Step 2: We will prove the convergence of $\tilde{\boldsymbol{\delta}}$ when $\tilde{\mathbf{s}} = \mathbf{0}$. Considering the following Lyapunov function candidate

$$V_2 = \frac{1}{2} \tilde{\boldsymbol{\delta}}^T \tilde{\boldsymbol{\delta}}. \quad (11)$$

Differentiating V_2 and using (8) yield

$$\begin{aligned} \dot{V}_2 &= \tilde{\boldsymbol{\delta}}^T \dot{\tilde{\boldsymbol{\delta}}} \\ &= -\tilde{\boldsymbol{\delta}}^T [\lambda_2 \tilde{\mathbf{s}} + \lambda_3 \boldsymbol{\sigma} + (\beta_d + \lambda_4) \text{sgn}(\boldsymbol{\sigma}) - \tilde{\boldsymbol{\delta}}] \\ &\quad \cdot -\lambda_2 \tilde{\boldsymbol{\delta}}^T \tilde{\mathbf{s}} - \lambda_3 \tilde{\boldsymbol{\delta}}^T \tilde{\boldsymbol{\delta}} - (\beta_d + \lambda_4) \|\tilde{\boldsymbol{\delta}}\| + \|\tilde{\boldsymbol{\delta}}\| \|\tilde{\boldsymbol{\delta}}\| \\ &\quad \cdot -\lambda_4 \|\tilde{\boldsymbol{\delta}}\| + \frac{\lambda_2}{2} \tilde{\mathbf{s}}^T \tilde{\mathbf{s}} \cdot -\lambda_4 \|\tilde{\boldsymbol{\delta}}\|. \end{aligned} \quad (12)$$

Eq.(12) indicates $\dot{V}_2 = -\sqrt{2}\lambda_4 V_2^{1/2}$. Therefore, the estimation error $\tilde{\boldsymbol{\delta}}$ finally converges to the origin in finite time

$T_d \cdot t_{d1} + \sqrt{2}V_2^{1/2}(0) / \lambda_4$, where $V_2(0)$ is the initial value of V_2 . The proof is completed.

2.3. ADSC Design

In this section, an ADSC is designed for DFFSM system (1) and (2). The control design procedure can be divided into the following two steps:

Step 1: Define the tracking error variable as

$$z_1 = x_e - x_{ed}. \quad (13)$$

Differentiating z_1 and using Property 1 yield

$$\dot{z}_1 = \dot{x}_e - \dot{x}_{ed} = J_g \dot{q} - \dot{x}_{ed} = Y_k(q, \dot{q}) \theta_k - \dot{x}_{ed}. \quad (14)$$

The parameter θ_k is unknown owing to kinematic uncertainties. We employ its estimation $\hat{\theta}_k$ to replace θ_k , that is, $\hat{x}_e = \hat{J}_g \dot{q} = Y_k(q, \dot{q}) \hat{\theta}_k$. Rewrite (14) as

$$\dot{z}_1 = \hat{J}_g^{-1} \dot{q} + Y_k(q, \dot{q}) \tilde{\theta}_k - \dot{x}_{ed} \quad (15)$$

where $\tilde{\theta}_k = \theta_k - \hat{\theta}_k$ represents the estimation error of θ_k . The virtual control α and the adaptive law of $\hat{\theta}_k$ are proposed as

$$\alpha = \hat{J}_g^{-1} (-c_1 z_1 + \dot{x}_{ed}), \quad (16)$$

$$\dot{\hat{\theta}}_k = \gamma_k \left[Y_k^T(q, \dot{q}) z_1 - \mu_k \hat{\theta}_k \right], \quad (17)$$

where c_1 , γ_k , μ_k are positive control gains. Substituting (16) into (15) yields

$$\begin{aligned} \dot{z}_1 &= \hat{J}_g \alpha + Y_k(q, \dot{q}) \tilde{\theta}_k - \dot{x}_{ed} + \hat{J}_g (\dot{q} - \alpha) \\ &= -c_1 z_1 + Y_k(q, \dot{q}) \tilde{\theta}_k + \hat{J}_g (\dot{q} - \alpha). \end{aligned} \quad (18)$$

Selecting a Lyapunov function candidate as

$$V_3 = \frac{1}{2} z_1^T z_1 + \frac{1}{2\gamma_k} \tilde{\theta}_k^T \tilde{\theta}_k, \quad (19)$$

The time derivative of V_3 is derived as

$$\begin{aligned} \dot{V}_3 &= z_1^T \dot{z}_1 + \frac{1}{\gamma_k} \tilde{\theta}_k^T \dot{\tilde{\theta}}_k \\ &= z_1^T \left[-c_1 z_1 + Y_k(q, \dot{q}) \tilde{\theta}_k + \hat{J}_g (\dot{q} - \alpha) \right] \\ &\quad - \tilde{\theta}_k^T \left[Y_k^T(q, \dot{q}) z_1 - \mu_k \hat{\theta}_k \right] \\ &= -c_1 z_1^T z_1 + z_1^T \hat{J}_g (\dot{q} - \alpha) + \mu_k \tilde{\theta}_k^T \hat{\theta}_k. \end{aligned} \quad (20)$$

To avoid using the time derivative of α in the following step, a first-order low-pass filter is given by

$$\gamma_\alpha \dot{\bar{\alpha}} + \bar{\alpha} = \alpha, \quad \bar{\alpha}(0) = \alpha(0) \quad (21)$$

where γ_α is the time constant.

Step 2: Introduce another error variable

$$z_2 = \dot{q} - \bar{\alpha}. \quad (22)$$

Define the filtering error as $\varepsilon_\alpha = \bar{\alpha} - \alpha$, the time derivative of ε_α can be expressed as

$$\dot{\varepsilon}_\alpha = \dot{\bar{\alpha}} - \dot{\alpha} = -\frac{1}{\gamma_\alpha} \varepsilon_\alpha + \phi(\square), \quad (23)$$

where $\phi(\square)$ is a continuous function consisting $\dot{\alpha}$, which is bounded by a positive constant, i.e., $\|\phi(\square)\| \leq \phi_M$. Using (4), the dynamics of z_2 is obtained as

$$\begin{aligned} M_0(q) \dot{z}_2 + C_0(q, \dot{q}) z_2 \\ = -M_0(q) \ddot{\bar{\alpha}} - C_0(q, \dot{q}) \bar{\alpha} + \tau + \delta. \end{aligned} \quad (24)$$

Design the control torque τ as

$$\tau = M_0(q) \ddot{\bar{\alpha}} + C_0(q, \dot{q}) \bar{\alpha} - \hat{J}_g z_1 - c_2 z_2 - \hat{\delta}, \quad (25)$$

Selecting another positive definite function

$$V_4 = V_3 + \frac{1}{2} z_2^T M_0(q) z_2 + \frac{1}{2} \varepsilon_\alpha^T \varepsilon_\alpha, \quad (26)$$

The time derivative of V_4 is calculated as

$$\begin{aligned} \dot{V}_4 &= \dot{V}_3 + z_2^T M_0(q) \dot{z}_2 + \frac{1}{2} z_2^T \dot{M}_0(q) z_2 + \varepsilon_\alpha^T \dot{\varepsilon}_\alpha \\ &\equiv -c_1 z_1^T z_1 + z_1^T \hat{J}_g (z_2 + \varepsilon_\alpha) + \mu_k \tilde{\theta}_k^T \hat{\theta}_k + z_2^T M_0(q) \dot{z}_2 \\ &\quad + \frac{1}{2} z_2^T \dot{M}_0(q) z_2 + \varepsilon_\alpha^T \dot{\varepsilon}_\alpha. \end{aligned} \quad (27)$$

Substituting (24) and (25) into (27) yields

$$\begin{aligned} \dot{V}_4 &\equiv -c_1 z_1^T z_1 - c_2 z_2^T z_2 - \frac{1}{\gamma_\alpha} \varepsilon_\alpha^T \varepsilon_\alpha + z_1^T \hat{J}_g \varepsilon_\alpha \\ &\quad + z_2^T \tilde{\delta} + \mu_k \tilde{\theta}_k^T \hat{\theta}_k + \varepsilon_\alpha^T \phi(\square). \end{aligned} \quad (28)$$

According to Young's inequality, one has

$$\begin{aligned} \dot{V}_4 &\leq -\left[c_1 - \frac{1}{2} \lambda_{\max}^2(\hat{J}_g) \right] z_1^T z_1 - \left(c_2 - \frac{1}{2} \right) z_2^T z_2 \\ &\quad - \left(\frac{1}{\gamma_\alpha} - 1 \right) \varepsilon_\alpha^T \varepsilon_\alpha - \frac{\mu_k}{2} \tilde{\theta}_k^T \tilde{\theta}_k + \frac{1}{2} \tilde{\delta}^T \tilde{\delta} + \eta. \end{aligned} \quad (29)$$

where $\eta = 0.5 \mu_k \theta_k^T \theta_k + 0.5 \phi_M^2$.

Theorem 2. For the DFFSM system (1) and (2), the tracking error z_1 in task space is uniformly ultimately bounded with the sliding mode disturbance observer (7), the virtual control (16), the adaptive law (17), and the control law (25).

Proof. According to Theorem 1, the estimation error $\tilde{\delta}$ will converge to zero after T_d , it is obtained that

$$\begin{aligned} \dot{V}_4 &\leq -\left[c_1 - \frac{1}{2} \lambda_{\max}^2(\hat{J}_g) \right] z_1^T z_1 - \left(c_2 - \frac{1}{2} \right) z_2^T z_2 \\ &\quad - \frac{\mu_k}{2} \tilde{\theta}_k^T \tilde{\theta}_k - \left(\frac{1}{\gamma_\alpha} - 1 \right) \varepsilon_\alpha^T \varepsilon_\alpha + \eta. \end{aligned} \quad (30)$$

By appropriate choosing gains such that $c_1 > 0.5 \lambda_{\max}^2(\hat{J}_g)$, $c_2 > 0.5$ and $\gamma_\alpha < 1$, Eq.(30) can be derived as

$$\dot{V}_4 \leq -\varsigma V_4 + \eta \quad (31)$$

with $\varsigma = \min\{\varsigma_0, \varsigma_1, \mu_k \gamma_k, 2\gamma_\alpha^{-1} - 2\}$, $\varsigma_0 = 2c_1 - \lambda_{\max}^2(\hat{J}_g)$, $\varsigma_1 = \lambda_{\max}^{-1}(M_0(q))(2c_2 - 1)$. From (31), the uniformly ultimate boundedness of z_1 , z_2 , $\tilde{\theta}_k$ and ε_α is verified. This completes the proof.

3. Numerical Simulations

In this section, numerical simulations with a planar 3-DOF DFFSM are constructed to verify the effectiveness of the proposed control scheme. The system parameters of the DFFSM are set as: $m_0 = 100\text{kg}$, $m_2^i = m_3^i = 2m_1^i = 10\text{kg}$, $I_0 = 10\text{kg}\cdot\text{m}^2$, $I_2^i = I_3^i = 2I_1^i = 0.1\text{kg}\cdot\text{m}^2$, $l_1^i = 0.2\text{m}$, $l_2^i = l_3^i = 0.75\text{m}$. The perturbed parts of inertial parameters are chosen as: $\Delta m_0 = 0.1m_0$, $\Delta m_j^i = 0.1m_j^i$, $\Delta I_0 = 0.1I_0$, $\Delta I_j^i = 0.1I_j^i$ ($i = a, b$, $j = 1, 2, 3$). The external disturbances exerted on the DFFSM system are:

$$d = [0.05 \sin(0.05t); 0.06 \cos(0.05t); 0.04 \sin(0.05t)]$$

The desired trajectories of each arm are (m):

$$\begin{aligned} x_{ed}^a &= 0.1\sin(0.1\pi t) + 0.1, & y_{ed}^a &= 0.1\cos(0.1\pi t) + 2.2, \\ x_{ed}^b &= 0.1\sin(0.1\pi t) - 0.1, & y_{ed}^b &= 0.1\cos(0.1\pi t) + 2.1. \end{aligned}$$

The control parameters of the disturbance observer (7), the virtual control (16), the adaptive law (17) and the control law (25) are chosen as: $\lambda_1 = 0.01$, $\lambda_2 = 1.5 \times 10^{-3}$, $\lambda_4 = 2\lambda_3 = 2 \times 10^{-3}$, $\gamma_k = \mu_k = 0.01$, $\gamma_\alpha = 0.1$, $c_1 = 5$, $c_2 = 1$. Damped least square method is utilized in (16) to avoid the possible dynamic singularity, that is, \hat{J}_g^{-1} is replaced by $\hat{J}_g^\# = (\lambda E + \hat{J}_g^T \hat{J}_g)^{-1} \hat{J}_g^T$, where $\lambda = 1 \times 10^{-3}$, E is the identity matrix.

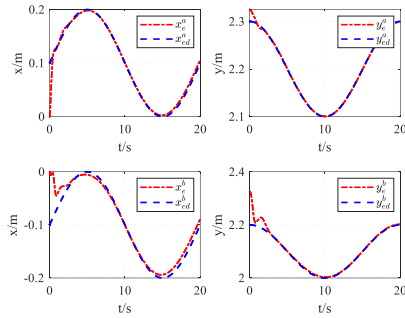


Fig.2 Time Response of x_e^i and x_d^i

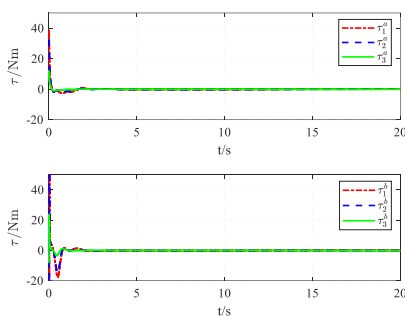


Fig.3 Time Response of τ^i

The simulation results are presented in Fig.2 and Fig.3. Fig.2 depicts the comparisons between the actual and desired trajectories of each arm. It is indicated that the actual trajectories could finally track the desired ones. The time vibrations of control input torque of each arm are shown in Fig.3. Thus, the robustness of the proposed ADSC with the sliding mode disturbance observer under disturbances and uncertainties is demonstrated.

4. Conclusions

This paper proposes a disturbance observer-based ADSC for DFFSM in task space subject to unknown disturbances, kinematic and dynamic uncertainties. It is proven that the uniformly ultimate boundedness of tracking errors is achieved with the proposed control scheme. In the future, the authors will study the coordinated control for DFFSM in on-orbit servicing.

Acknowledgements

This work was supported in part by the NSFC (62227810, 62133001) and the National Basic Research Program of China (973 Program: 2012CB821200, 2012CB821201).

References

1. L. Yan, H. Yuan, W. Xu, et al, Generalized relative Jacobian matrix of space robot for dual-arm coordinated capture, *Journal of Guidance, Control, and Dynamics*, Vol. 41(5), 2018, pp.1202-1208.
2. L. Shi, S. Kayastha, J. Katupitiya, Robust coordinated control of a dual-arm space robot, *Acta Astronautica*, Vol. 138, 2017, pp.475-489.
3. L. Shi, H. Jayakody, J. Katupitiya, et al, Coordinated control of a dual-arm space robot: Novel models and simulations for robotic control methods, *IEEE Robotics & Automation Magazine*, Vol. 25(4), 2018, pp.86-95.
4. C. Yang, Y. Jiang, J. Na, et al, Finite-time convergence adaptive fuzzy control for dual-arm robot with unknown kinematics and dynamics, *IEEE Transactions on Fuzzy Systems*, Vol. 27(3), 2019, pp.574-588.
5. J. Cheng, L. Chen, The fuzzy neural network control scheme with H_∞ tracking characteristic of space robot system with dual-arm after capturing a spin spacecraft, *IEEE/CAA Journal of Automatica Sinica*, Vol. 7(5), 2020, pp.1417-1424.
6. Y. Liu, W. Yan, T. Zhang, et al, Trajectory tracking for a dual-arm free-floating space robot with a class of general nonsingular predefined-time terminal sliding mode, *IEEE Transactions on Systems, Man, and Cybernetics: Systems*, Vol. 52(5), 2021, pp.3273-3286.

Authors Introduction

Ms. Qian Sun



She received the B.S. degree in Automation from Chongqing University, Chongqing, China, in 2020. She is currently working toward the Ph.D. degree in control theory and control engineering from Beihang University, Beijing, China. Her research interests include coordinated control of on-orbit servicing.

Prof. Yingmin Jia



He received B.S. degree from Shandong University, Jinan, China, in 1982, and the M.S. and Ph.D. degrees from Beihang University, Beijing, China, in 1990 and 1993, respectively. He is currently a professor with the Seventh Research Division and the director of the Center for Information and Control at Beihang University. His research interests include robust control, robotic systems, spacecraft coordination and on-orbit servicing.